



Published in final edited form as:

J Appl Microbiol. 2015 November ; 119(5): 1403–1411. doi:10.1111/jam.12940.

A new small molecule inhibits *Streptococcus mutans* biofilms in vitro and in vivo

Wenting Pan¹, Mingwen Fan¹, Hui Wu², Christian Melander³, and Chang Liu^{1,*}

¹The State Key Laboratory Breeding Base of Basic Science of Stomatology (Hubei-Most) & Key Laboratory for Oral Biomedical Engineering of Ministry of Education, School & Hospital of Stomatology, Wuhan University, 237 Luoyu Road, Wuhan 430079, China

² Department of Pediatric Dentistry, UAB School of Dentistry, Birmingham, Alabama 35294, USA

³ Department of Chemistry, North Carolina State University, Raleigh, North Carolina 276952, USA

Abstract

Aims—The aim of this study is to identify new small molecules that can inhibit *Streptococcus mutans* biofilms by *in-vitro* and *in-vivo* model.

Methods and Results—We evaluated the effect of a small molecule 2-amino-imidazole/triazole conjugate (2-AI/T) on the formation of *S. mutans* biofilms by culturing in 96-well plates. Toxicity was assessed through cell culture and intragastrically administering to mice. The anti-biofilm and anti-caries effects were investigated *in vivo*. The inhibitive mechanism was detected by isobaric tag for relative and absolute quantitation (iTRAQ) and RT-QPCR. *In vitro* and *in vivo* study revealed that 2-AI/T significantly inhibited biofilm formation of *S. mutans* and is more so than inhibiting planktonic cells without toxicity. The ribosome and histidine metabolism pathways of *S. mutans* were significantly regulated by this compound.

Conclusions—These results suggest that the 2-AI/T conjugate is a potent inhibitor that can be potentially developed into a new drug to treat and prevent dental caries.

Significance and Impact of the Study—This is the first study to use small molecule from marine natural products, to protect from dental caries *in vivo*. It has potential broad range application in clinical caries prevention, or as a bioactive ingredient for food applications.

Keywords

antimicrobials; biofilm; *Streptococci*; dental caries; small molecule

*Chang Liu (Corresponding author) The State Key Laboratory Breeding Base of Basic Science of Stomatology (Hubei-Most) & Key Laboratory for Oral Biomedical Engineering of Ministry of Education, School & Hospital of Stomatology, Wuhan University, 237 Luoyu Road, Wuhan 430079, China. Tel.: +862785615341, liuc0728@whu.edu.cn.

Conflict of interest

No conflict of interests.

Introduction

Bacterial biofilms are bacterial communities encased in a protective matrix, within which provides a more stable environment, thus within the biofilms bacteria are more resistant to environmental stresses including traditional antibiotics (Musk and Hergenrother 2006). Therefore it is important to develop new inhibitors targeting bacterial biofilms. Small molecules derived from marine natural products have diverse biological activities. These activities are used by marine organisms as offensive weapons for predation or defense weapons for their protection, and they become a potential resource for discovery of new activities that interfere with invading microbes (Skropeta and Wei 2014). Small molecules analogues of bromoageliferin and oroidin, which were isolated from the marine sponge *Agelas coniferas*, inhibit biofilm formation by *Pseudomonas aeruginosa* (Huigens *et al.* 2007). Oroidin derivatives not only inhibit biofilm formation, but also disperse preformed biofilms of common proteobacteria (Ballard *et al.* 2009).

Dental caries, the most common oral infectious disease, is initiated by interaction of the cariogenic bacterium *S. mutans* with host, environmental, and nutritional factors. Although mechanical removal and antibiotics treatment are commonly used in dental practices, new prevention and therapeutics against this pathogen are still needed due to persistent colonization of *S. mutans* on the tooth surface by tenacious biofilms. Our group aims to develop new small molecules to inhibit *S. mutans* biofilms.

Recently, a lot of studies have focusing on evaluating the secondary metabolites containing the 2-aminoimidazole (2-AI) moiety for their anti-biofilm activities (Richards *et al.* 2008; Forte *et al.* 2009; Al-Mourabit *et al.* 2011; Yeagley *et al.* 2012; Jiao *et al.* 2013). The 2-AI derivatives are promising precursors to derive more potent new broader spectrum antimicrobial drugs. For example, Reed *et al.* synthesized and assembled a new 2-AI molecule library based on 2-AI and identified compounds that specifically inhibit biofilm formation of *E. coli* (Reed *et al.* 2010). Using a similar approach, we have identified a diverse group of 2-AI derivatives that target biofilm formation by *S. mutans* in a multispecies biofilm (Liu *et al.* 2011).

Based on this 2-AI structure, a variety of 2-AI/T have been designed by attaching a triazole group to the tail group of the 2-AI (Reyes *et al.* 2011). A 2-AI/T derivative was identified that inhibits biofilm formation by pathogens such as *Acinetobacter baumannii* and methicillin-resistant *Staphylococcus aureus* (Rogers *et al.* 2010; Su *et al.* 2011)). Using a number of 2-AI derivatives we identified a 2-AI/T *S. mutans* biofilm inhibitor (Fig. 1). In this study, we further evaluated its efficacy and mechanism, which provided us useful information for our future evaluation of the compound for clinical application.

Materials and methods

Bacterial strains, culture conditions, and chemicals

S. mutans UA159 was grown statically at 37 °C on Mitis-Slivan-Bacitracin (MSB, Difco Laboratories) agar plate under an aerobic atmosphere with 5% CO₂. A single colony of UA159 was inoculated into 4 ml brain-heart infusion (BHI) broth (Becton-Dickinson, USA)

and grown overnight. Then the overnight culture was inoculated into fresh BHI to allow bacteria to grow until they reached exponential growth phase at an optical density at 470 nm (OD_{470}) of 0.8. The exponentially grown bacteria were used for biofilm assays. *S. mutans* biofilms were grown in a chemically defined medium: biofilm medium (BM) containing 1% sucrose (Loo *et al.* 2000). Synthesized compound 2-AI/T was dissolved in dimethyl sulfoxide (DMSO) at different concentrations and arrayed in a 96-well flat-bottom polystyrene microtiter plates (Nalge Nunc International, Rochester, NY) for testing.

Biofilm inhibitory assays and CLSM analysis

S. mutans grown at the exponential phase, was inoculated into 96-well plate with different concentration gradients ($6.25 \mu\text{mol l}^{-1}$ to $100 \mu\text{mol l}^{-1}$) of 2-AI/T. The biofilms treated with 2-AI/T at its IC_{50} concentration (concentration at which 50% biofilm inhibition occurs) were stained with live/dead BacLight bacterial viability kit (Invitrogen, USA). Staining and other experimental procedures followed our previous studies (Liu *et al.* 2011).

Metabolic activity assay of biofilm and planktonic *S. mutans* cells

To measure the metabolic activity of biofilm cells, *S. mutans* grown at the exponential phase and 2-AI/T were added into 96-well plates and incubated at 37°C with 5% CO_2 to allow biofilms to develop. At time points of 4 h, 6 h, 8 h, 10 h, 12 h, 24 h after incubation, planktonic cells were removed from the 96-well plates, and cell metabolic activity of the attached biofilm cells was quantified by using MTT method. Staining of the biofilms at different time points was measured at 490 nm (OD_{490}) using a microplate reader (BioTek ELx). 100 μl of planktonic cell suspension removed from each well of the biofilms was diluted into 900 μl PBS individually. Half of the diluent was used to determine bacterial colony forming units (CFU). The other half was used to assess metabolic activity of the planktonic cells. Results were given as percentages of planktonic cell activity applying the following formula: % activity = $\text{Log CFU test} \times \text{Log CFU}^{-1} \text{ control} \times 100$.

Cytotoxicity assay

Healthy gum tissue from crown lengthening surgery was collected (inclusion criteria: surgical dental gum color normal, no bleeding on probing, no attachment loss, periodontal pocket depth is less than 2 mm, no loose teeth, no alveolar bone on X-ray film absorbent), then cultured in Dulbecco's modification of Eagle's medium (DMEM) with 10% fetal calf serum (FBS) and 100 U ml^{-1} penicillin and 100 $\mu\text{g ml}^{-1}$ streptomycin at 37°C with 5% CO_2 . For cellular analyses, 80% confluency cells at passages 4-7 were seeded into 96-well plates containing 2-AI/T at different concentrations, and the viability for gingival fibroblasts was measured by MTT. The experiment was carried out in triple wells, and repeated three times.

Acute toxicity assay

Twenty specific pathogen-free (SPF) female mice at six week provided by the Medical Laboratory Animal Center of Wuhan University were divided into two groups randomly. One group was intragastrically administrated 2-AI/T 5000 mg kg^{-1} while the other group administered DMSO, a solvent for 2-AI/T, as control. The two groups were observed for

two weeks on autonomic activity, stress response, body weight, and appetite. Blood and urine were taken and biochemical tests were performed to determine the levels of glutamic-pyruvic transaminase, glutamic-oxalacetic trans-aminease, blood glucose, total bilirubin, urea nitrogen, and serum creatinine. All animal model experiments were approved by Medical ethics committee of Wuhan University.

Anti-biofilm *in vivo* in a mouse model

A mouse colonization model was first used to evaluate anti-biofilm efficacy. Thirty SPF female mice at the six-week age were randomly divided into two groups, 2-AI/T treated and untreated group, and each group split for three sub-groups which contained five mice respectively, labeled day1, day3, day5. These mice were fed by diet with appropriate antibiotics (ampicillin, chloramphenicol, and carbencillin 1.0 g kg⁻¹ diet) for three consecutive days. Then 2×10⁹ CFU ml⁻¹ of *S. mutans* UA159 were inoculated onto the teeth of mice for three times in the morning, while in the afternoon, 2-AI/T at its IC₅₀ or DMSO was inoculated firstly, then *S. mutans* was inoculated for twice. The interval of each time is 30 min. Those operations continued for three days. All the groups were provided caries-promoting diet Keyes 2000# (Keyes 1958). To confirm effective inoculation and bacterial colonization, cotton swab samples of the animals' teeth were collected on day 1, 3 and 5 after the last inoculation. The samples were appropriately diluted, and spread onto MSB agar plates to count colony forming units of *S. mutans*. Each sample was diluted into three concentration gradients, with three repeated plates at each concentration.

Anti-caries *in vivo* in a rat model

A rat model based on the anti-caries vaccine model our groups have used before was established with some modifications (Liu *et al.* 2008). The same antibiotic regimen as the mouse anti-biofilm model was used to treat SPF female SD rats at 18-day age for four days. Then the bacterial inoculation and administration of 2-AI/T as described for the mouse model was carried out for four days. On the next day post-infection, swab samples were collected and spread onto MSB agar plates to verify bacterial colonization. Forty days post-infection, the rats were sacrificed, and their mandible middle molars were removed and subsequently processed for micro computed tomography (micro-CT). Using 3D imaging, and cross-sectional diagram analysis, defective volumes on hard tissue of teeth from different groups were evaluated and calculated.

Protein extraction and iTRAQ analysis

S. mutans was inoculated at 1:100 dilutions to obtain biofilms as previously described and biofilms were scraped from 6-well-plates. Those biofilm samples were mixed with lysis buffer and then sonicated for 5 min. Proteins were collected by centrifugation and cell debris were discarded. DTT was added to the supernatant to a final concentration of 10 mmol l⁻¹, incubated for 1h at 56 °C. Then IAM was added quickly till the final concentration was 55 mmol l⁻¹, keeping still for 1 h at room temperature. The protein was washed and its concentration was determined using Bradford protein assay. 100 µg protein samples was digested and labeled with iTRAQ reagent (8 plex multiplex kit Applied Biosystem. Part No.4381663) follow the instruction. We set two groups and each repeating

once, resulting in four tags labeling of iTRAQ reagents (iTRAQ reporter ions of 115, 116, 117, 118 mass/charge ratio). Those labeled samples were pooled and fractionated by HPLC column, then analyzed by tandem mass spectrometry (MS/MS). To identify and quantify the protein, the 2.3.0 version of mascot software was used and database searching was made against swissprot_bacteria. To retrieve taxonomic hierarchy and bioinformatics analysis, Kyoto Encyclopedia of Genes and Genomes (KEGG) pathways in each group were determined based on swissprot_bacteria database.

Expression of pathway-associated genes by *S. mutans*

Overnight cultures of *S. mutans* UA159 were inoculated as described in itraq section. Total RNA was extracted according to the protocol previously described (Liu *et al.* 2011). cDNA samples were analyzed by using SYBR green PCR supermix (Roche, Basel, Switzerland) and specific primers on 7900 Real Time PCR system (Applied Biosystems). PCR primers are listed in Table 1. The PCR cycle used was set up as follows: 40 cycles of 95 °C for 15 s and 60 °C for 1 min. After the last cycle, the reaction mixtures were kept at 95 °C and then 55 °C for 1 min each, followed by a slow ramp from 95 °C for 15 s, 60 °C for 15 s, 95 °C for 15 s. RNA samples without reverse transcription were used as negative controls to ensure no contamination by genomic DNA. Relative expression levels of all selected genes were normalized using 16S rRNA as an internal standard. All results were repeated independently for three times.

Statistical analysis

Experimental data were analyzed on SPSS 18.0 software (SPSS Inc., Chicago, IL), plotted with Origin8.0 software and presented as means \pm standard deviation. Comparisons between two groups were calculated using Student's *t*-test. *P* value < 0.05 was considered statistically significant.

Results

Effect of 2-AI/T on *S. mutans* biofilms

Effect of 2-AI/T on biofilm formation of *S. mutans* was first examined by assessing biofilm biomass using crystal violet staining. 2-AI/T dose dependently inhibited crystal violet staining, indicating inhibition of biofilm formation by 2-AI/T. As shown in Fig. 2, 2-AI/T at 12.5 $\mu\text{mol l}^{-1}$ or higher significantly reduced biofilm formation. The IC_{50} of the compound was determined to be around 75 $\mu\text{mol l}^{-1}$ by SPSS 18.0.

To characterize the effect further, we evaluated biofilm structure using CLSM. Wild type *S. mutans* displayed as a dense and thick biomass with illegible outline, while 2-AI/T treated, biofilm microcolonies were altered, in which *S. mutans* cells were loosely aggregated. In the Z series analysis, it is apparent that bacterial biofilms treated with 2-AI/T became much sparser and thinner than the control group, indicating effectiveness of the compound on altering biofilm structures (Fig. 3).

Effect of 2-AI/T on metabolic activity

MTT has been used to measure bacterial viability within biofilm cells. The value of the 2-AI/T treated group was significant lower than that of the control groups ($P < 0.05$) in the consecutive 24 hs. No difference ($P > 0.05$) is observed between the blank group and the control group (Fig. 4A). For *S. mutans* planktonic cells, there was no difference in CFU value between 2-AI/T treated and the control groups at 24 h (Fig. 4B). Within 24 hs, the metabolic activity of *S. mutans* biofilm cells was sustained, while the activity of planktonic cells dramatically declined in the first 10 h but sharply rose in the next 14 h until achieving the same state as the control group.

Cytotoxicity *in vitro* and acute toxicity of 2-AI/T in animal model

To determine the safe dose of 2-AI/T, we carried out toxicity assays using various concentrations of 2-AI-T. In cytotoxicity tests using human gingival fibroblasts as a cell model, we determined that 2-AI/T at up to $100 \mu\text{mol l}^{-1}$ did not affect growth of human gingival fibroblasts ($P > 0.05$) (Fig. 5A). To further evaluate the toxicity of the compound, we performed acute toxicity tests in an *in vivo* animal model. As shown in Fig. 5B, no difference in all biochemical parameters is evident between the treated and control group, suggesting no effect of the compound on animal physiology.

2-AI/T inhibited bacterial colonization and reduced caries incidence *in vivo*

Two animal models were used to assess the effect of 2-AI/T on bacterial colonization. Within the experimental time frame, the *S. mutans* control group displayed a significant increase in CFUs, while in the group treated with 2-AI/T, growth of *S. mutans* exhibited a stagnancy. A significant difference ($P < 0.05$) between the two groups was shown,, indicating the anti-biofilm effect of 2-AI/T *in vivo* (Fig. 6A).

In a rat models of anti-caries study, the remaining teeth volume data were obtained by micro-CT scanning (Fig. 6B). The bars suggested there was significant differences between 2-AI/T group and control group ($P < 0.05$). Crowns from animals treated with 2-AI/T displayed less carious defect upon exposed to a cariogenic environment.

2-AI/T altered expression profiles of some proteins and genes

Parameters for quantitative analysis were set up as follows: median used as protein ratio type and normalization method; Minimum peptides were 1; P value < 0.05 ; fold difference > 1.2 . According to this, 394 proteins have differences, including 188 up-regulated proteins and 206 down-regulated proteins. KEGG revealed that proteins were involved in 56 signaling pathways. Among those pathways, ribosome protein metabolism ($P = 2.395e-05$) and histidine metabolism ($P = 0.020$) pathways had significant differences. To confirm the result, mRNA expression of the most different proteins involved in these two pathways were detected by real-time QPCR. The expressions of *rplB* and *rpsQ* of ribosome protein metabolism were down-regulated while the expressions of *hisD* and *hisH* genes of histidine metabolism were up-regulated significantly compared with the control groups.

Discussion

In this study, we chose a new small molecule 2-AI/T and determined that it could effectively inhibit biofilm formation by the cariogenic bacterium *S. mutans*. Continuously, we detected bacterial metabolic activity after co-culture with 2-AI/T for 24 h. Within 24 h, *S. mutans* biofilm cell was sustained, while the activity of planktonic cell was dramatically declined in the first 10 h but sharply risen in the next 14 h until got the same state as control group. However, we were pleased to find that it has better inhibitory effect towards biofilm cells rather than planktonic cells. The results may be explained that 2-AI/T adsorbed in biofilm, a relatively enclosed environment, has difficulty diffusing, leading to a longer duration of action and promoting bacterial metabolic changes; or it is because 2-AI/T has two different mechanisms towards these two states of bacteria (Doron *et al.* 2001; Tam *et al.* 2006). What we can confirm is 2-AI/T has longer inhibitory effect towards biofilm cell rather than planktonic cell, and it requires us to further investigate the inhibitory mechanisms.

Pharmaceutical safety was evaluated by *in vitro* and *in vivo* testing. Many studies have shown the strong correlation between *in vitro* cytotoxicity and *in vivo* animal experiments (Barile and Cardona 1998; Dierickx 2000). In *in vitro* experiments, we aimed to assess whether 2-AI/T in the concentration range that effectively inhibited bacteria biofilm can affect the oral tissues. So rather than using common commercialized oral cancer cell lines or immortalized oral epithelial cell lines, we chose to use primary human gingival fibroblast as a model (Ahn *et al.* 2012). The experiment determined that there was no cytotoxicity of this compound. In acute toxicity experiments, we selected the blood biochemical index to evaluate the organ function in mice. Serum BUN (blood urea nitrogen) and CR (creatinine) are indicators of renal function. BUN and CR levels are inversely associated with the renal function. ALT and AST were used to assess the function of the liver. The malfunction of the liver is associated with increases in the levels of these two enzymes (Wang *et al.* 2006). Blood sugar levels may also reflect liver function and basic metabolism in mice. When the bile duct is obstructed or loses function, total bilirubin increases to reflect the structural hepatobiliary disease. Therefore, this experiment selected five commonly used biochemical indicators to assess the acute toxicity (Thanabhorn *et al.* 2006). Experimental results showed that 2-AI/T had no effect on the organ function.

Since we developed 2-AI/T to use as a shield after toothbrushing for a long-term effect against caries, the animal model for anti-biofilm and anti-caries are necessary. We designed our *in vivo* anti-biofilm model, with some modifications according to Simone's group (Simionato *et al.* 2006). In order to mimic the clinical application, we inoculated *S. mutans* first, then after 4 h treated with 2-AI/T. Instead of killing the mice, we chose to use a cotton swab directly to sample the bacteria. It was worth noting that there was a sustained inhibitive effect of 2-AI/T *in vivo*. A related study concerning the effect of tea components on *S. mutans* biofilms demonstrated that potential mechanisms of action involved modification of cell surface properties and blockade of proteins from interacting with surfaces (Wang *et al.* 2013). It also can permeate into membrane and interact with biofilm associated proteins (Thompson *et al.* 2012). Further studies are actually in progress in order to define the mechanism of action of the compound.

There have been several studies concerning anti-caries effects of natural compounds. Ikeno and Otake administered polyphenols extracted from tea and propolis into the water to feed rats, and demonstrated effectiveness of these nature products against dental caries using the rat model (Ikeno *et al.* 1991; Otake *et al.* 1991). In our study, we explored suitable bacterial concentrations and times for continuous inoculation based on the anti-biofilm model, and extended the experimental time frame to 70 days after we inoculated bacteria. Compared with classic caries scoring, micro-CT, which we chose in the study, does not require destruction of the dental structure, as well as staining which could raise the rate of omissions and errors.

The mechanism indicates that ribosomal protein and histidine metabolism are involved in this compound's effect on *S. mutans*. As we know, ribosomal proteins can interact with some virulence factors to influence cell growth and division of *S. mutans* (Mattos-Graner *et al.* 2006). Wilkins also found that with the growth rate of *S. mutans* in the acidic medium was reduced, the ribosomal protein S1P were down-regulated (Wilkins *et al.* 2002). While, histidine is involved in a wide array of metabolic processes including ammonia, glutamate, and a one-carbon compound (Bender 2012). In 1980s, MacKay suggested that salivary histidine-rich polypeptides could inhibit or kill *S. mutans*, both serotype b and c strains (MacKay *et al.* 1984), which is consistent with our observation. In the pathway of histidine metabolism, urocanase plays an important role. Cabral reported that urocanase could be a new target to inhibit the biofilm formation of *Acinetobacter baumannii* (Cabral *et al.* 2011).

In conclusion, our studies have identified the small molecule 2-AI/T, which effectively inhibits *S. mutans* biofilms. Also, we revealed the mechanism of its inhibitive effects. These results offers a new possibility for oral anti-caries prevention.

Acknowledgments

This work was supported by NIH/NIDCR grant R01 DE022350 (HW) and NSFC 81201260 (CL).

References

- Ahn SJ, Cho EJ, Kim HJ, Park SN, Lim YK, Kook JK. The antimicrobial effects of deglycyrrhizinated licorice root extract on *Streptococcus mutans* UA159 in both planktonic and biofilm cultures. *Anaerobe*. 2012; 18:590–596. [PubMed: 23123832]
- Al-Mourabit A, Zancanella MA, Tilvi S, Romo D. Biosynthesis, asymmetric synthesis, and pharmacology, including cellular targets, of the pyrrole-2-aminoimidazole marine alkaloids. *Nat Prod Rep*. 2011; 28:1229–1260. [PubMed: 21556392]
- Ballard TE, Richards JJ, Aquino A, Reed CS, Melander C. Antibiofilm activity of a diverse oroidin library generated through reductive acylation. *J Org Chem*. 2009; 74
- Barile FA, Cardona M. Acute cytotoxicity testing with cultured human lung and dermal cells. *In Vitro Cell Dev Biol Anim*. 1998; 34:631–635. [PubMed: 9769147]
- Bender RA. Regulation of the histidine utilization (hut) system in bacteria. *Microbiol Mol Biol Rev*. 2012; 76:565–584. [PubMed: 22933560]
- Cabral MP, Soares NC, Aranda J, Parreira JR, Rumbo C, Poza M, Valle J, Calamia V, Lasa I, Bou G. Proteomic and functional analyses reveal a unique lifestyle for *Acinetobacter baumannii* biofilms and a key role for histidine metabolism. *J Proteome Res*. 2011; 10:3399–3417. [PubMed: 21612302]

- Dierickx PJ. Cytotoxicity of the MEIC reference chemicals in rat hepatoma-derived Fa32 cells. *Toxicology*. 2000; 150:159–169. [PubMed: 10996672]
- Doron S, Friedman M, Falach M, Sadovnic E, Zvia H. Antibacterial effect of parabens against planktonic and biofilm *Streptococcus sobrinus*. *Int J Antimicrob Agents*. 2001; 18:575–578. [PubMed: 11738348]
- Forte B, Malgesini B, Piutti C, Quartieri F, Scolaro A, Papeo G. A submarine journey: the pyrrole-imidazole alkaloids. *Mar Drugs*. 2009; 7:705–753. [PubMed: 20098608]
- Huigens RW, Richards JJ, Parise G, Ballard TE, Zeng W, Deora R, Melander C. Inhibition of *Pseudomonas aeruginosa* biofilm formation with Bromoageliferin analogues. *J Am Chem Soc*. 2007; 129:6966–6967. [PubMed: 17500516]
- Ikeno K, Ikeno T, Miyazawa C. Effects of propolis on dental caries in rats. *Caries Res*. 1991; 25:347–351. [PubMed: 1836157]
- Jiao W, Zhang F, Zhao X, Hu J, Suh JW. A novel alkaloid from marine-derived actinomycete *Streptomyces xinghaiensis* with broad-spectrum antibacterial and cytotoxic activities. *PLoS One*. 2013; 8:e75994. [PubMed: 24098415]
- Keyes PH. Dental caries in the molar teeth of rats. I. Distribution of lesions induced by high-carbohydrate low-fat diets. *J Dent Res*. 1958; 37:1077–1087. [PubMed: 13611122]
- Liu C, Fan M, Bian Z, Chen Z, Li Y. Effects of targeted fusion anti-caries DNA vaccine pGJA-P/VAX in rats with caries. *Vaccine*. 2008; 26:6685–6689. [PubMed: 18789994]
- Liu C, Worthington RJ, Melander C, Wu H. A new small molecule specifically inhibits the cariogenic bacterium *Streptococcus mutans* in multispecies biofilms. *Antimicrob Agents Chemother*. 2011; 55:2679–2687. [PubMed: 21402858]
- Loo CY, Corliss DA, Ganeshkumar N. *Streptococcus gordonii* biofilm formation: identification of genes that code for biofilm phenotypes. *J Bacteriol*. 2000; 182:1374–1382. [PubMed: 10671461]
- MacKay BJ, Denepitiya L, Iacono VJ, Krost SB, Pollock JJ. Growth-inhibitory and bactericidal effects of human parotid salivary histidine-rich polypeptides on *Streptococcus mutans*. *Infect Immun*. 1984; 44:695–701. [PubMed: 6724693]
- Mattos-Graner RO, Porter KA, Smith DJ, Hosogi Y, Duncan MJ. Functional analysis of glucan binding protein B from *Streptococcus mutans*. *J Bacteriol*. 2006; 188:3813–3825. [PubMed: 16707674]
- Musk DJ Jr, Hergenrother PJ. Chemical countermeasures for the control of bacterial biofilms: effective compounds and promising targets. *Curr Med Chem*. 2006; 13:2163–2177. [PubMed: 16918346]
- Otake S, Makimura M, Kuroki T, Nishihara Y, Hirasawa M. Anticaries effects of polyphenolic compounds from Japanese green tea. *Caries Res*. 1991; 25:438–443. [PubMed: 1667297]
- Reed CS, Huigens RW 3rd, Rogers SA, Melander C. Modulating the development of *E. coli* biofilms with 2-aminoimidazoles. *Bioorg Med Chem Lett*. 2010; 20:6310–6312. [PubMed: 20846860]
- Reyes S, Huigens RW, Su Z, Simon ML, Melander C. Synthesis and biological activity of 2-aminoimidazole triazoles accessed by Suzuki-Miyaura cross-coupling. *Org Biomol Chem*. 2011; 9:3041–3049. [PubMed: 21394327]
- Richards JJ, Ballard TE, Melander C. Inhibition and dispersion of *Pseudomonas aeruginosa* biofilms with reverse amide 2-aminoimidazole oroidin analogues. *Org Biomol Chem*. 2008; 6:1356–1363. [PubMed: 18385842]
- Rogers SA, Bero JD, Melander C. Chemical synthesis and biological screening of 2-aminoimidazole-based bacterial and fungal antibiofilm agents. *Chembiochem*. 2010; 11:396–410. [PubMed: 20049758]
- Simionato MR, Tucker CM, Kuboniwa M, Lamont G, Demuth DR, Tribble GD, Lamont RJ. *Porphyromonas gingivalis* genes involved in community development with *Streptococcus gordonii*. *Infect Immun*. 2006; 74:6419–6428. [PubMed: 16923784]
- Skropeta D, Wei L. Recent advances in deep-sea natural products. *Nat Prod Rep*. 2014; 31:999–1025. [PubMed: 24871201]
- Su Z, Peng L, Worthington RJ, Melander C. Evaluation of 4,5-disubstituted-2-aminoimidazole-triazole conjugates for antibiofilm/antibiotic resensitization activity against MRSA and *Acinetobacter baumannii*. *ChemMedChem*. 2011; 6:2243–2251. [PubMed: 21928438]

- Tam A, Shemesh M, Wormser U, Sintov A, Steinberg D. Effect of different iodine formulations on the expression and activity of *Streptococcus mutans* glucosyltransferase and fructosyltransferase in biofilm and planktonic environments. *J Antimicrob Chemother.* 2006; 57:865–871. [PubMed: 16549514]
- Thanabhorn S, Jaijoy K, Thamaree S, Ingkaninan K, Panthong A. Acute and subacute toxicity study of the ethanol extract from *Lonicera japonica* Thunb. *J Ethnopharmacol.* 2006; 107:370–373. [PubMed: 16697541]
- Thompson RJ, Bobay BG, Stowe SD, Olson AL, Peng L, Su Z, Actis LA, Melander C, Cavanagh J. Identification of BfmR, a response regulator involved in biofilm development, as a target for a 2-Aminoimidazole-based antibiofilm agent. *Biochemistry.* 2012; 51:9776–9778. [PubMed: 23186243]
- Wang B, Feng WY, Wang TC, Jia G, Wang M, Shi JW, Zhang F, Zhao YL, Chai ZF. Acute toxicity of nano- and micro-scale zinc powder in healthy adult mice. *Toxicol Lett.* 2006; 161:115–123. [PubMed: 16165331]
- Wang Y, Lee SM, Dykes GA. Potential mechanisms for the effects of tea extracts on the attachment, biofilm formation and cell size of *Streptococcus mutans*. *Biofouling.* 2013; 29:307–318. [PubMed: 23528127]
- Wilkins JC, Homer KA, Beighton D. Analysis of *Streptococcus mutans* proteins modulated by culture under acidic conditions. *Appl Environ Microbiol.* 2002; 68:2382–2390. [PubMed: 11976112]
- Yeagley AA, Su Z, McCullough KD, Worthington RJ, Melander C. N-substituted 2-aminoimidazole inhibitors of MRSA biofilm formation accessed through direct 1,3-bis(tert-butoxycarbonyl)guanidine cyclization. *Org Biomol Chem.* 2012; 11:130–137. [PubMed: 23076976]

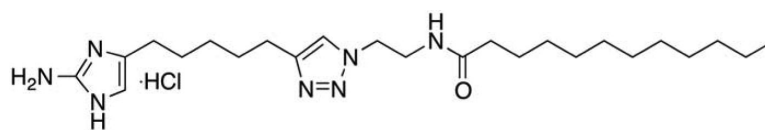


Figure 1.
The structure of small molecule 2-AI/T.

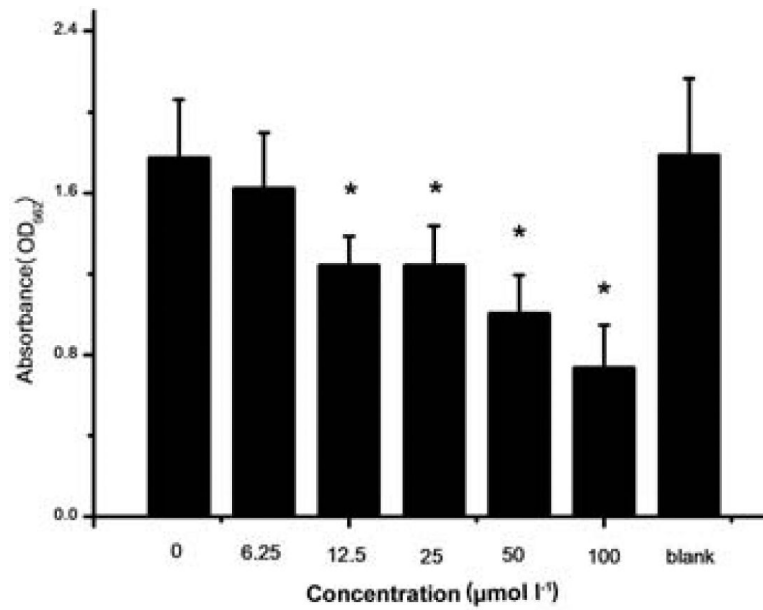


Figure 2.

Effect of 2-AI/T on biofilm formation. *S. mutans* was treated with 2-AI/T in different concentrations and the control group was treated with DMSO, a solvent of 2-AI/T. Values represent the means \pm standard deviations from three independent experiments. Asterisks and number signs demonstrated significant differences between groups ($P < 0.05$).

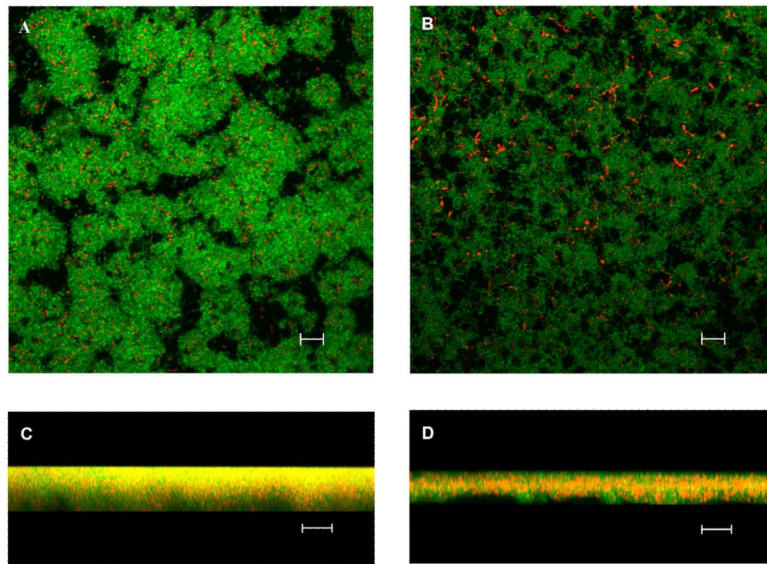


Figure 3. Biofilm structures were analyzed by confocal laser scanning microscopy. The left panels represent biofilms treated with DMSO 16 h with 40X objective, and the right panels represent biofilms treated with 2-AI/T 16 h with 40X objective. The top views (A, B) and vertical sections (C, D) of the biofilms are depicted. The scale bar is 10 μm .

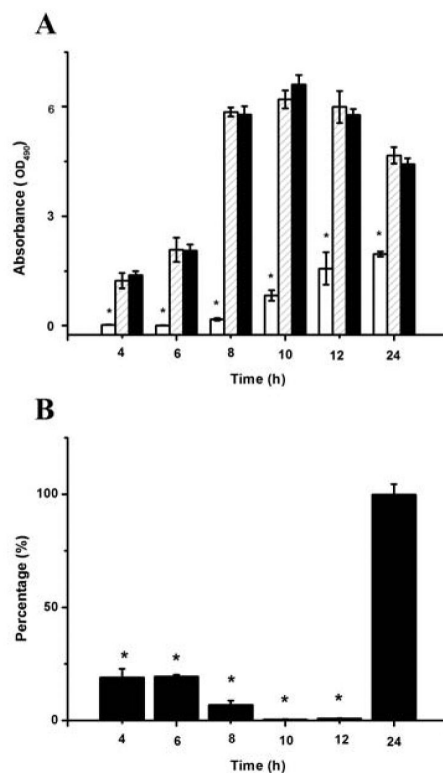


Figure 4.

Effect of 2-AI/T on metabolic activity of biofilm cells and planktonic cells. Biofilm cells on the bottom of wells were detected by MTT (A). Planktonic cells grown in culture media away from the biofilm surface was harvested and used to determine CFU. The percentage of CFU was calculated by comparing treated groups with DMSO control groups (100%) (B). Values represent the means \pm standard deviations from three independent experiments. Asterisks and number signs demonstrated significant differences between groups ($P < 0.05$). In figure 4A: (****) 2AI/T, (*****) DMSO and (*****) Control.

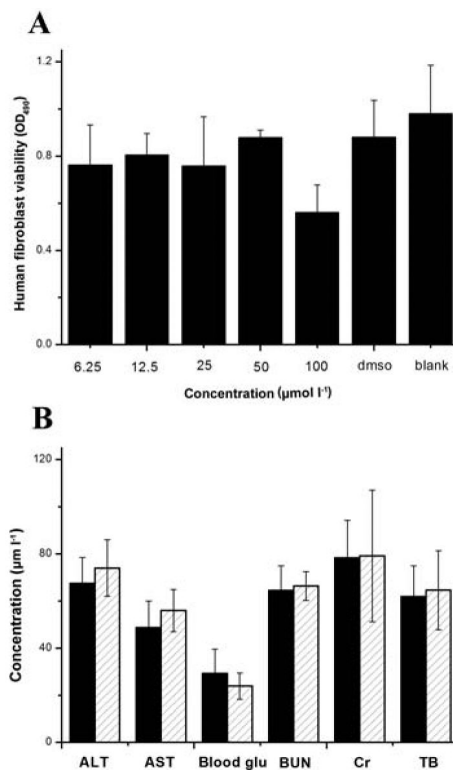


Figure 5.

Cytotoxicity of 2-AI/T on human gingival fibroblast (A) and acute toxicity of 2-AI/T in mice was measured by blood levels of substances (B). Values represent the means \pm standard deviations from three independent experiments. ALT: glutamic-pyruvic transaminase, AST: glutamic-oxalacetic transaminase, BUN: blood urine nitrogen, Cr: serum creatinine level, TB: total bilirubin blood level. In figure 5B: (*****)DMSO and (*****) 2AI/T).

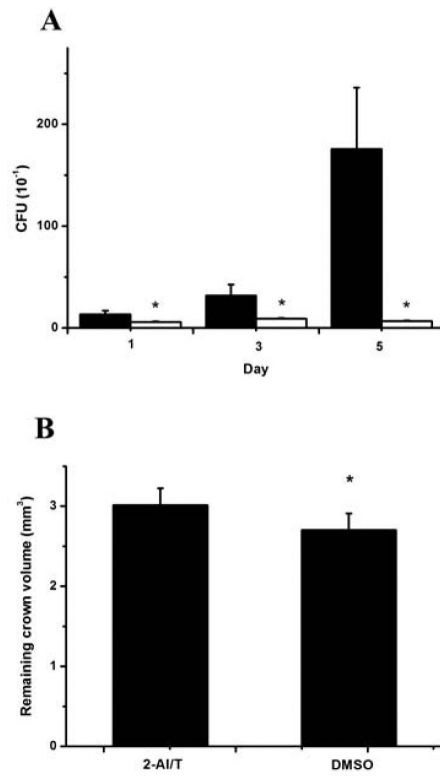


Figure 6. Effect of 2-AIT on *S. mutans* biofilm *in vivo* (A) and carious study (B). Values represent the means \pm standard deviations. Asterisks and number signs demonstrated significant differences between groups ($P < 0.05$). In figure 6A: (*****) DMSO and (*****) 2AIT.

Table 1

Primer sequence used in the real-time RT-PCR and genes' expression folds

Gene	Primer sequence (5'-3')		Expression fold
	Forward primer	Reverse primer	mean±sd
rplB	CAACCGCCTCAACGCCATCTT	CGGTCGCATTACTGTTCG TCATCA	0.1145±0.0694
rpsQ	TGTTGCTGAAAGCGGACGAGTTT	GCTAGTTGGTCGTGTTGT GTCTGA	0.0027±0.0004
hisD	CTGATTTCGTCCTTGGAGC	TGATTTCTTTCACACCAG CA	2.9729±0.2626
hisH	TGATTACGACGCAGGCAATA	CTGGAAAGGCACCAACT CCT	1.4088±0.3310
16S rRNA	CCTACGGGAGGCAGCAGTAG	CAACAGAGCTTTACGATC CGAAA	

Author Manuscript

Author Manuscript

Author Manuscript

Author Manuscript